

LEED and Auger electron spectroscopy study of the Si(111)-2×1 + Ag overlayer system in the temperature range 8–300 K and coverage range $\theta = 0-20$ monolayers

V. Yu. Aristov, I. L. Bolotin, F. A. Grazhulis, and V. M. Zhilin

Institute of Solid State Physics, Academy of Sciences of the USSR

(Submitted 30 January 1986)

Zh. Eksp. Teor. Fiz. **91**, 1411–1426 (October 1986)

Low energy electron diffraction (LEED) and Auger electron spectroscopy (AES) are used to study the growth processes of Ag films on an initially clean Si(111)-2×1 surface and the evolution of the samples during heating to room temperature after decomposition of Ag at 8 K. It is observed that in the case of deposition at 8 K the distribution of the Ag atoms over the thickness of the films is statistical, and the atoms form highly disordered ultrathin Ag films with a short-range-order length $\xi \approx 3a_{Ag}$, where a_{Ag} is the crystallographic lattice constant of the Ag. Upon heating of Ag films prepared at 8 K a number of phase transitions are observed in the neighborhood of $T \approx 100$ K; these are manifested by the appearance of the LEED structures Ag(111)-1×1, Si(111)-3×1-Ag, and Si(111)- $\sqrt{7} \times \sqrt{7}R(\pm 19.1^\circ)$ -Ag against a uniform ($\theta \leq 3$) or a nonuniform ($\theta \geq 3-4$) background. Low-temperature deposition of Ag on the Si(111)-2×1 surface has little effect on the 2×1 superstructure, but subsequent heating of the sample to $T \approx 100$ K leads to the transition Si(111)-2×1 → Si(111)-1×1 at $\theta \approx 0.4-0.5$. This transition is due to a sharp increase in the strength of the interaction between the Ag atoms and the Si(111) surface when the temperature T is raised (at $T \approx 100$ K.) The mean free path in silver is determined for electrons of energy 92 eV ($4.4 \pm 1.4 \text{ \AA}$) and 356 eV ($6 \pm 1.7 \text{ \AA}$).

I. INTRODUCTION

Practically all investigations of the adsorption of Ag atoms on an Si(111) surface have been carried out at relatively high temperatures, $T \approx 300$ K. (To the best of our knowledge, this can be said of almost all investigations of metal-atom adsorption on semiconductor surfaces). In contrast to the system Si(111)-7×7 + Ag, for which there are a rather large number of publications (see, e.g., the review (Ref. 1) and also Refs. 2–14), relatively little work has been reported on the system Si(111)-2×1 + Ag (Refs. 15–21).

Studies of the adsorption of Ag atoms on an Si(111)-2×1 surface at 300 K have shown that the initial 2×1 superstructure superreflection remains qualitatively unchanged to $\theta \approx 0.3$ [θ is the coverage in monolayers, with one monolayer corresponding to a number of Ag atoms equal to the number of Si atoms on the (111) surface, $7.8 \cdot 10^{14} \text{ cm}^{-2}$]. For $\theta \geq 0.3$ a new structure, Si(111)- $\sqrt{7} \times \sqrt{7}R(19.1^\circ)$ begins to form.¹⁷ The extra LEED spots from the $\sqrt{7} \times \sqrt{7}$ superstructure are the most intense at a coverage $\theta \approx 2/3$, at which point there is a break in the curve of the intensity $I_{Si}(\theta)$ of the Si LVV Auger peak (92 eV). The diffraction beams from the 2×1 and $\sqrt{7} \times \sqrt{7}$ structures are simultaneously visible up to $\theta \approx 2$. For $\theta > 2$ only the Si(111) 1×1 and the Ag(111) reflections are visible. The latter have begun to form already at $\theta \approx 1$ (Ref. 17) or $\theta \approx 0.5$ (Ref. 19). There is no consensus as to the growth mechanism of the Ag film on the Si(111)-2×1 surface at room temperature. In fact, it has been assumed^{1,9,22,23} that at $T \approx 300$ K the growth of the Ag film on the Si(111)-2×1 surface proceeds by the Frank–Van der Merwe mechanism (Fig. 1a). On the other hand there are

investigations in which other growth mechanisms have been proposed (see Ref. 1, and works cited therein), namely, the Stranski-Krastanov and the Volmer-Weber mechanisms (Figs. 1b and 1c).

Until recently it has been believed that in the Ag-Si system at 300 K there is no characteristic intermixing of the metal and the semiconductor atoms.^{16,24} However, the authors of Ref. 18, on the basis of their experiments, have concluded that at room temperature (in contrast to the situation at liquid nitrogen temperature) the Ag and Si atoms intermix to some extent to a depth of two monolayers of the sili-

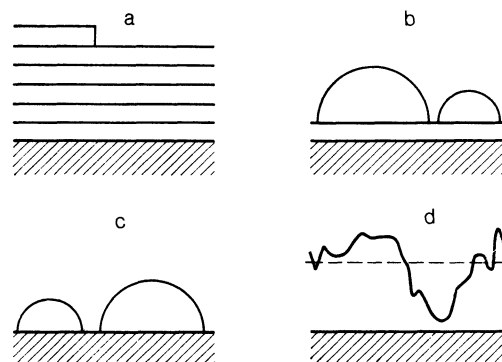


FIG. 1. Schematic representation of film growth mechanisms. a) Frank–Van der Merwe—the growth of each successive monolayer begins after the previous one is completed; b) Stranski-Krastanov—upon completion of the growth of the first monolayer three-dimensional (3D) islands grow; c) Volmer-Werner—the growth of 3D islands; d) model of the statistical growth of a film on a substrate cooled to liquid helium temperatures.

con substrate. Model calculations²⁵ also suggest the formation of a surface with embedded atoms.

A comparison of investigations on the system Si(111)-Ag that have been carried out at room temperature and above shows that a reduction of the temperature from, say, $T \approx 600$ to $T \approx 300$ K can lead to marked changes in the structures of the Si(111)-Ag interface and in the growth mechanism. Accordingly, there is a great deal of interest in analogous investigations at lower temperatures, near that of liquid helium (see also Ref. 26). We believe that such investigations may cast additional light on the results of "high temperature" ($T \approx 300$ K) studies. In view of these considerations we have used the methods of Auger electron spectroscopy (AES) and low energy electron diffraction (LEED) to study the system Si(111)-Ag in the initial stages of coverage of the initially clean Si(111)- 2×1 surface by Ag atoms at temperatures 8–300 K.

II. EXPERIMENTAL METHOD AND SAMPLES

The experiments were conducted with the use of an ESCALAB-5 system, having a hemispherical electron energy analyzer and a two-grid LEED system. The base pressure was $5 \cdot 10^{-11}$ Torr and during the experiment it did not exceed $(2 - 4) \cdot 10^{-10}$ Torr. In order to achieve the low temperatures (to 8 K) a special attachment similar to that described in Ref. 27 was developed which made it possible to change samples without breaking vacuum. The sample temperature could be controlled in the range 8–300 K, and it was measured with a carbon resistance thermometer that was attached to a similar sample on the same sample holder. The error in the temperature measurements was less than 1%.

Silver (purity 99.9999 at%) was evaporated from a pre-outgassed tantalum wire heated by an electric current. The relative current stability during the evaporation was better than $5 \cdot 10^{-5}$. After proper outgassing of the silver source turning it on had no effect on the vacuum. The deposition rate was controlled in the range 10^{-4} – $5 \cdot 10^{-2}$ Å/s, and it was measured directly with a quartz crystal thickness monitor during deposition of the silver on the sample. The flux of Ag atoms was incident at an angle $\approx 20^\circ$ to the normal to the sample surface. The operation of the thickness monitor was checked both by the total evaporation of known weights and by the linearity of the monitor reading with time during the evaporation. The rms deviation from linearity did not exceed $\Delta\theta \approx 0.07$. Although the flux of atoms was very stable during the deposition, the absolute value of θ could have a systematic deviation 30% high or low from the values quoted in this paper because of possible errors in calibration of the thickness matter. The Auger spectra showed that the deposited films were free of impurities to the limits of sensitivity of the spectrometer.

In the experiments we used *p*-type silicon with a doping impurity concentration $\sim 10^{13}$ and $\sim 10^{18}$ cm⁻³, and *n*-type silicon with an impurity concentration $\sim 10^{-13}$ and $\sim 10^{17}$ cm⁻³. The samples were cleaved at room temperature along the (111) plane in the $\langle 211 \rangle$ direction with two wedges (wedge angles 90 and 30°) inserted into slots in opposite sides of the sample. The geometry of the sample made it

possible to make three 10×6 mm cleavages. More than 80 cleavages were studied in the experiments. As a rule a cleavage contained a number of specularly smooth areas separated by visually distinct steps. During the measurements the probing electron beam was attuned to one of the specular areas. The geometry of the apparatus permitted the Auger spectra to be taken during the deposition without changing the position of the sample. Most of the Auger spectra were taken with a primary beam energy of 3 kV. The amplitudes of the 92 eV Silicon *L* *VV* peak and of the 356 eV silver *M* *VV* peak were measured.

The LEED pattern was obtained with a standard two-grid analyzer in the ESCALAB-5 system. The primary electron beam energy was varied from 30–120 eV, and the beam was incident within a few degrees of normal to the sample surface. The LEED pattern was recorded with a photographic film. The intensity profiles of the diffracted beams were determined by photometry of the negatives.

Generally, the experiments were conducted in the following way. The sample was cleaved in a vacuum $\sim 10^{-10}$ Torr at room temperature. When a good cleaved surface was obtained the Ag was deposited on the sample, which was kept at room temperature or at 8 K. In the latter case the sample was cooled after cleaving to 8 K. Next, during the deposition of the Ag atoms, the Auger spectra were taken and the LEED patterns were recorded at various stages of coverage θ . At the desired thickness the deposition was stopped and the samples were heated to room temperature. At the same time, the Auger spectra were taken and the LEED patterns were recorded, but now as functions of temperature at constant coverage θ . Sometimes this procedure was repeated with additional cycles of cooling and heating.

In the case of deposition at room temperature the Auger spectra were also taken and the LEED patterns were recorded as functions of the coverage. Some samples, that reached a specified coverage, were studied by the same methods, but as functions of temperature while cooling to 8 K and subsequent heating to room temperature.

III. EXPERIMENTAL RESULTS

A. Auger electron spectroscopy

1. Deposition at 8 K

Typical curves of the amplitudes I_{Si} and I_{Ag} of the Auger 92-eV Si peak and the 356 eV Ag peak as functions of θ , taken at low temperatures, are shown in Figs. 2 and 3. The ratio $I_{\text{Ag}}/I_{\text{Si}}$ as a function of θ is shown in Fig. 4.

The behavior of the Si(111)-Ag system as the sample temperature is raised in the interval 8–300 K after low-temperature deposition depends strongly on the coverage θ . The intensity ratio of the Auger peaks for $\theta \leq 1$ is unchanged within experimental error as the sample is heated. On the other hand, for samples with $\theta > 1$ the ratio $I_{\text{Ag}}/I_{\text{Si}}$ begins to decrease irreversibly at $T \approx 100$ K. We found that, after the sample has reached room temperature, the greater the coverage θ the smaller this ratio compared to the initial ratio at 8 K, and it decreases by about two orders of magnitude for $\theta \approx 15$. It was found that this intensity-ratio change occurs in

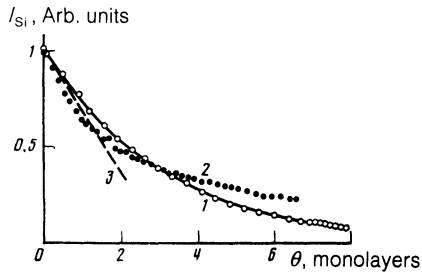


FIG. 2. Si Auger signal amplitude as a function of the coverage θ : 1) at $T = 8$ K; 2) at room temperature; the solid line corresponds to growth according to formula (1); 3) tangent to the calculated curve at the point $\theta = 0$.

a wide temperature range, 100–350 K. We stress that the characteristic temperature T^* at which these changes begin to be noticeable increases with increasing coverage. For example, this temperature is $T^* \approx 200$ K for $\theta \approx 4$ and $T^* \approx 340$ K for $\theta \approx 15$.

2. Deposition at room temperature

The dependence of the Si and Ag Auger signal amplitudes at room temperature on θ in the coverage range $\theta \approx 0$ to 1 is essentially linear (see Figs. 2 and 3), a result that agrees with the results of other authors.^{16,17,19} For Si this dependence is steeper than that for $T = 8$ K. Both curves have a kink near $\theta \approx 1$ and then they slope more gently than for $T = 8$ K. The difference in the ratio I_{Ag}/I_{Si} for $\theta \geq 3$ is especially pronounced (Fig. 4); whereas at 8 K the ratio I_{Ag}/I_{Si} depends approximately exponentially on θ over the entire range from $\theta \approx 0$ to 15, at room temperature, as can be seen from Fig. 4, it can be regarded as a linear function of θ from $\theta \approx 3$ to $\theta \approx 10$. For $\theta \geq 10$ the slope decreases. As a result, for $\theta \approx 15$ the ratios I_{Ag}/I_{Si} for samples on which Ag was deposited at 300 and 8 K differ by two orders of magnitude.

Cooling to 8 K samples that have been prepared at room temperature and reheating to room temperature has practically no effect on the amplitudes of the Auger spectra.

B. Low energy electron diffraction

The LEED patterns from the clean silicon (111) surfaces cleaved at room temperature usually showed a single-domain Si(111)- 2×1 superstructure. This structure re-

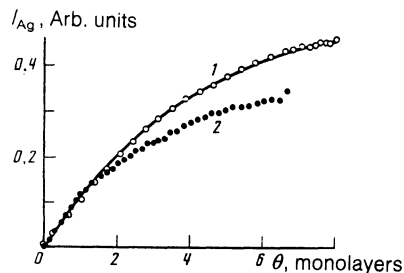


FIG. 3. Ag Auger signal amplitude as a function of the coverage θ : 1) at $T = 8$ K; 2) at room temperature. The solid line corresponds to the calculation from formula (2).

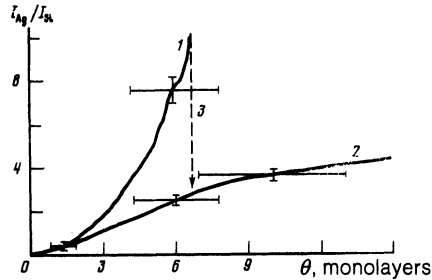


FIG. 4. Ratio of the silver and silicon Auger signal amplitudes: 1) at 8 K; 2) at room temperature; 3) the change in the ratio during heating to room temperature a sample with a film prepared at 8 K.

mained unchanged when the samples were cooled to 8 K, in agreement with the results of Refs. 28 and 29. The superstructure diffracted beams were sharp and were in the $\langle 211 \rangle$ direction.

During the deposition of the silver on the cleaved silicon surface we observed, depending on θ and T , a large variety of LEED patterns corresponding to the structure Si(111)- 2×1 , Si(111)- $\sqrt{7} \times \sqrt{7} R (\pm 19.1^\circ)$, and a three-domain Si(111)- 3×1 plus Ag(111)- 1×1 structure, and at $\theta \approx 1.2$ – 1.3 , if the deposition was carried out at room temperature, we were able to see all three of these structures at once (see Fig. 5a). We point out that Fig. 5b shows the diffraction pattern obtained after deposition of Ag to $\theta \approx 0.7$ – 0.8 with subsequent heating of the samples to room temperature, while Fig. 5c shows nominally how the diffracted beams are arranged for the various structures depicted in Figs. 5a and 5b.

For a more compact exposition, the main results obtained in this investigation are gathered in Table I, which shows the regions of existence of the several structures as functions of the coverage θ of silver, the deposition temperature, and other factors.

We shall now turn to a more detailed description and discussion of the experimental LEED results.

1. Deposition at 8 K

Beginning with the very lowest coverages $\theta \ll 1$, a uniform increase in the LEED background intensity is observed up to the point where it saturates to some extent at $\theta \geq 3$. At the same time the contrast of the diffraction beams from the Si(111)- 2×1 structure decreases (the intensities of the main beams and the extra superstructure beams decrease by essentially the same amount). At $\theta \approx 3$ all the diffracted beams from the Si(111)- 2×1 structure disappear, but the enhanced intensity in the vicinity of the specular, 00 beam remains. For $\theta \geq 3$ – 4 the background becomes nonuniform: some increase in intensity is observed at which would be the reflections of the Ag(111) film. The size of each spot is commensurate with the spot separation (strong smearing). With increasing θ the spots become stronger and smaller.

2. Heating the samples after deposition at 8 K

Coverage range $\theta = 3$ to 4. For $\theta < 0.4$ – 0.5 the Si(111)- 2×1 structure remains when the sample is heated to room

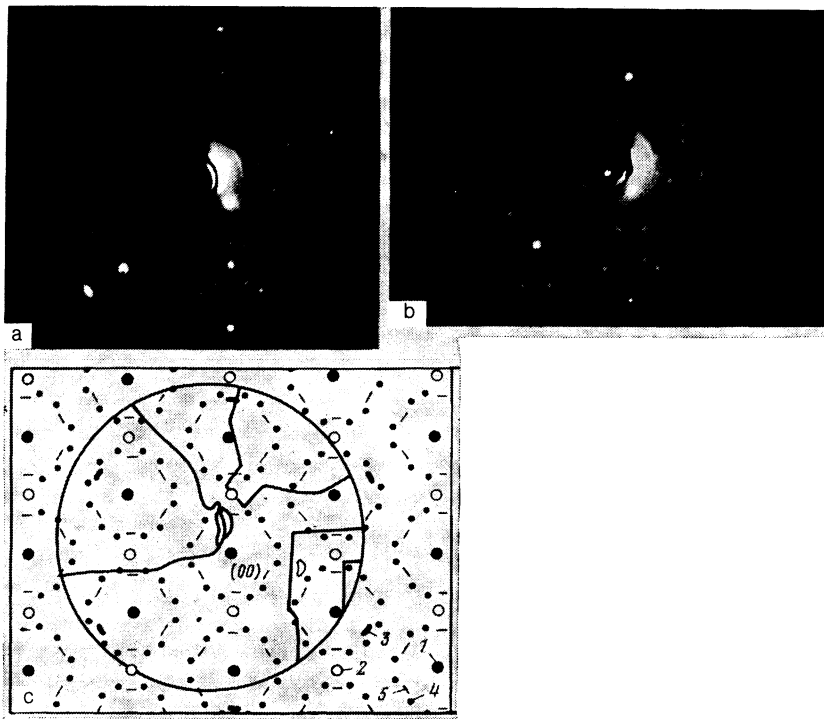


FIG. 5. LEED pattern of a cleaved Si(111) surface after depositing silver: a) deposition at room temperature, $\theta = 1.25$, primary beam energy $E_p = 38$ eV; b) deposition at 8 K with subsequent heating to room temperature, $\theta = 0.75$, $E_p = 41$ eV; c) arrangement of the diffracted beams of the various structures: 1) Si(111)- 1×1 ; 2) Si(111)- 2×1 ; 3) Ag(111)- 1×1 ; 4) Si(111)- $\sqrt{7} \times \sqrt{7}R (\pm 19.1^\circ)$ -Ag; 5) Si(111)- 3×1 -Ag.

temperature. For $\theta \geq 0.4-0.5$ the extra diffracted beams from the Si(111)- 2×1 superstructure disappear during the heating, that is, a $2 \times 1 \rightarrow 1 \times 1$ transition takes place. The temperature of this transition becomes lower as the coverage is increased. For $\theta \approx 0.5, 0.7$, and 1, the transition temperature is, respectively, near 230, 180, and 130 K. Thus, a structural transition, Si(111)- $2 \times 1 \rightarrow$ Si(111)- 1×1 , occurs during heating when the coverage is greater than some critical value, $\theta^* \approx 0.4-0.5$.

Within the coverage range that we studied we observed

three more structures that appeared during heating of the samples.

a) For $0.2-0.3 \leq \theta \leq 1$ regions of enhanced intensity appear against the uniform background of the LEED pattern, beginning at $T \approx 130$ K, and with further heating they become sharp and bright diffraction beams of the Si(111)- $\sqrt{7} \times \sqrt{7}R (\pm 19.1^\circ)$ structure (see Fig. 5b). The diffracted beams of this structure show up sharpest at $\theta \approx 0.7-0.8$.

b) In the range $0.7 \leq \theta \leq 3-4$, during heating of the sam-

TABLE I. Main experimental results: ranges of silver coverage and other conditions for observation of the LEED patterns.

Experimental conditions	Si(111)- 2×1	Si(111)- 1×1	Si(111)- $\sqrt{7} \times \sqrt{7}R (\pm 19.1^\circ)$	Si(111)- 3×1	Ag(111)- 1×1	Background
Deposited at room temperature	$0 \leq \theta \leq 2$	$2 \leq \theta \leq 22$ or higher	$0.2-0.3 \leq \theta \leq 2.5$, most clearly visible for $\theta \approx 1.2-1.3$	$0.5 \leq \theta \leq 3-6$	$\theta \geq 0.5$	weak
Deposited at 8 K	$0 \leq \theta \leq 3$	not observed	not observed	not observed	not observed	1) grow strongly up to $\theta \leq 3-4$, uniform 2) appear in regions of enhanced intensity for $\theta \geq 3-4$
Heating to room temperature	1. Remains for $\theta \leq 0.4-0.5$ 2. Undergoes $2 \times 1 \rightarrow 1 \times 1$ transformation	appears out of the background of the 2×1 structure for $\theta \geq 0.4-0.5$	appears out of the background in the form of diffuse spots, $0.2-0.3 \leq \theta \leq 1$	appears out of the background as rings, which turn into diffracted beams which divide into separate diffracted beams	appears out of: 1) a uniform background at $0.7 \leq \theta \leq 3-4$; 2) regions of enhanced intensity for $3-4 < \theta \leq 12$	fades out and transforms into other structures
Observation at room temperature after heating	$0 \leq \theta < 0.5$	$0.4-0.5 \leq \theta \leq 11$ or higher	$0.2-0.3 \leq \theta \leq 1$	$0.7 \leq \theta \leq 2-4$	$\theta \geq 0.7$	weak
Notes			structure sensitive to vacuum conditions; not observed for $p \geq 3 \cdot 10^{-10}$ Torr	evidently due to double diffraction	beams somewhat smeared out around the circumference	

ples and beginning at $T \approx 100$ K, rings of radius equal to one-third the distance between the Si(111)- 1×1 beams are gradually formed around the Si(111)- 1×1 beams. With further heating the rings separate into six beams, smeared over the circumference of the circle and lying in the directions of the nearest Si(111)- 1×1 diffracted beams (see Fig. 5c), i.e., the Si(111)- 3×1 structure is formed. The brightest beams of the Si(111)- 3×1 structure are formed around the 00 beam. For $\theta \gtrsim 2$ the intensities of the 3×1 beams decrease with increasing θ and for $\theta \gtrsim 4$ they are practically invisible.

c) During heating of samples with $\theta \gtrsim 0.7$, Ag(111)- 1×1 beams are gradually formed out of the uniform LEED background at $T \gtrsim 100$ K. During the formation of this pattern, spots of enhanced intensity appear first, and then as the temperature is increased they decrease in area and increase in brightness. When room temperature is reached the radial diffuseness of the spots is much less than the circumferential diffuseness, which can be as much as $\pm 15^\circ$. The amount of radial and circumferential diffuseness decreases with increasing θ . The orientation of the Ag(111)- 1×1 diffracted beams that are formed correlates with the crystallographic directions of the Si(111) substrate plane. This means that the same crystallographic directions of the Si(111)- 1×1 and Ag(111)- 1×1 structures coincide and the distances between neighboring beams are in the ratio 3:4, respectively, for the two structures.

The range of θ from 3–4 to 11. As mentioned above, during deposition at 8 K to coverages $\theta \gtrsim 3-4$ "spots" of enhanced intensity appear in the LEED pattern. As the coverage is increased to $\theta \approx 10$ the spots become much more conspicuous, but they remain quite diffuse (see above). Heating of the samples prepared in this way with $3-4 \leq \theta \leq 11$ (samples with $\theta > 11$ were not studied) does not produce any marked changes in the LEED pattern up to $T \approx 100$ K. With further heating of the samples the spots become brighter and smaller. The spots gradually turn into the diffracted beams of the Ag(111)- 1×1 structure mentioned above, and the overall background is reduced. This process for $\theta \approx 9$ is illustrated in Fig. 6.

At higher temperatures (relative to the temperature at

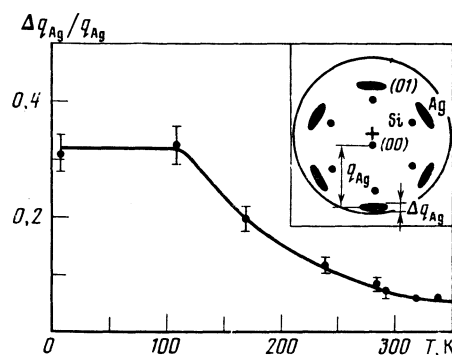


FIG. 6. Relative half width of the (01) diffracted beam from silver, measured in the radial direction ($E_p = 70$ eV) for $\theta = 9$, as a function of the annealing temperature. The inset is a diagram that shows how q_{Ag} and Δq_{Ag} are defined. The cross shows the center of the screen; the primary beam is incident at an angle of 2° from the normal to the sample.

which the Ag diffracted beams are formed) the Si(111)- 1×1 beams become visible. For example, for samples with $\theta \approx 9$ the temperature for the formation of the Si(111)- 1×1 diffracted beams is in the region of 280 K. We have found that this temperature increases with the coverage, but we did not make any detailed studies of this effect. In sum, after heating to room temperature samples with $\theta \approx 3-11$ the Si(111)- 1×1 structure is always seen in addition to the Ag(111)- 1×1 structure.

3. Deposition at room temperature

The characteristic ranges of θ in which one or another of the structures are observed in the process of deposition at room temperature are given in Table I. We note that the Si(111)- $\sqrt{7} \times \sqrt{7} R (\pm 19.1^\circ)$ is sharpest for $\theta \approx 1.2-1.3$. Our LEED results that we show in Table I for the Si(111)-Ag system prepared by deposition at room temperature agree on the whole with the results in Refs. 17 and 19, and we shall therefore not dwell at length on the results of the "high temperature" investigations, noting only that, in contrast to Refs. 17 and 19, we observed by LEED the Si(111)- 3×1 structure. The only experiment known to us in which this structure has been observed in deposition at room temperature onto the cleaved Si surface at room temperature used the method of reflection high-energy electron diffraction.²³

In conclusion we call attention to the following. All the LEED patterns that we have observed at room temperature, regardless of whether they were obtained by deposition on surfaces at 8 K and heated to room temperature or deposited on surfaces at room temperature, remained unchanged when the samples were subsequently cooled to 8 K. The increased contrast of the diffraction spots after cooling was evidently in consequence of the Debye-Waller factor. Heating the samples again produced no noticeable changes in the LEED pattern.

IV. DISCUSSION OF THE RESULTS

The adsorption of Ag atoms, having a temperature $T \approx 1000$ K during evaporation, onto a cold (≈ 10 K substrate is characterized by: 1) a high rate of cooling of the atoms upon adsorption³⁰ and 2) the absence of surface or bulk diffusion or interchange of the adsorbing atoms with the atoms of the substrate.³¹ The last, by itself, is a consequence of the absence of diffusion.

For such an adsorption process one would expect, first, an atomically sharp interface between the metal and semiconductor, and second, a film without an island structure but having a continuous thickness over the whole surface because of the statistical nature of the distribution of the atoms. The latter expectation will be correct if an atom that has "fallen" on the surface does not change its position.

The high rate of cooling of the atoms and the absence of diffusion may lead to the formation of a highly nonequilibrium structure of both the surface and the film. Generally speaking, in the state of the surface and the film a broad spectrum is possible between the two extremes: amorphous and monocrystalline.

Guided by the above-mentioned observations, we shall

determine the coverage dependence of the intensities of the silver and silicon Auger spectra for the case of low-temperature deposition. We shall thus assume that the Ag film is formed with a Poisson distribution of atoms over the thickness of the film.

$$P_m = \frac{(\alpha\theta)^m}{m!} \exp(-\alpha\theta),$$

where m is the number of atoms located one over the other in a surface adsorption site the size of which is the order of the lattice constant, p_m is the probability of this confirmation, θ is the average thickness of the film (expressed in monolayers), and $\alpha \approx 0.56$ is a factor that is equal to the ratio of the density of Si atoms in the Si(111) plane to the density of Ag atoms in the Ag(111) plane (we assume that at 8 K the spacings between the Ag atoms are the same as in Ag metal). The Poisson distribution, strictly speaking, assumes statistical independence of the spatial distribution of the Ag atoms and at the same time implies that the film is amorphous. However, the pattern of the atoms distribution does not really change qualitatively for the case of weak correlation effects due to the motion of the impinging Ag atoms on the surface over distances no greater than the lattice constant. Assuming that a film of constant thickness d_0 attenuates an electron beam of energy ε by an amount $\exp(d_0/l)$, where $l = l(\varepsilon)$ is the effective inelastic mean free path of an electron of energy ε and without energy loss, we obtain from the Poisson distribution expressions for the intensities $I_{\text{Si}}(\theta)$ and $I_{\text{Ag}}(\theta)$:

$$I_{\text{Si}} \propto \exp\{-\alpha\theta[1 - \exp(-1/l(\varepsilon_1))]\}, \quad (1)$$

$$I_{\text{Ag}} \propto 1 - \exp\{-\alpha\theta[1 - \exp(-1/l(\varepsilon_2))]\}, \quad (2)$$

where ε_1 is 92 eV and ε_2 is 356 eV and $l(\varepsilon)$ is in units of d , where d is the average distance between neighboring Ag atoms. For $l(\varepsilon) \gg 1$, expressions (1) and (2) simplify, since $\exp(-1/l(\varepsilon)) \approx 1 - 1/l(\varepsilon)$. In this case we obtain

$$I_{\text{Si}} \propto \exp\{-\alpha\theta/l(\varepsilon_1)\}, \quad (3)$$

$$I_{\text{Ag}} \propto 1 - \exp\{-\alpha\theta/l(\varepsilon_2)\}. \quad (4)$$

It should be emphasized that generally speaking, it is not *a priori* obvious that expressions of type (1) and (2) are valid for arbitrary values of θ , since it is not clear that one can in fact use the same parameter l for both $\theta \lesssim 1$ and $\theta \gtrsim 1$. This issue can only be resolved by a comparison of expressions (1) and (2) with experimental data. Before making such a comparison, let us note also the following.

It is clear that the density of a nonequilibrium film must be different from that of crystalline silver, but we have no data available on the density of the nonequilibrium films that we have produced, since the methods that we use allow us to determine only the mass of silver per unit area. Therefore we shall assume that the average distance between the silver atoms in the film is independent of the substrate structure and is approximately equal to the spacing in crystalline silver. Under this assumption a single monolayer of Ag on the surface should correspond to $\alpha\theta = 1$, i.e., a monolayer corresponds to $\theta \approx 1.8$, since $\alpha \approx 0.56$.

As can be seen from Figs. 2 and 3, the experimental Auger spectroscopy results obtained at 8 K are in good agreement with dependences of the type (1) and (2) if $l(\varepsilon_1) = 1.5 \pm 0.5$ and $l(\varepsilon_2) = 2 \pm 0.6$ for all values of θ . Taking the average distance between monolayers to be equal to the average distance d between Ag atoms in the crystalline state ($d \approx 2.9$ Å) we obtain for the average film thickness $\langle d_0 \rangle = d\alpha\theta$ and for the inelastic mean free path in the Ag film we obtain $dl(\varepsilon_1) = 4.4 \pm 1.4$ Å and $dl(\varepsilon_2) = 6.0 \pm 1.7$ Å.

The results of the low-temperature LEED measurements show, first of all, that deposition of Ag atoms in 8 K has little effect on the Si(111)- 2×1 superstructure. This result suggests the following conclusion: that at 8 K the adsorbed Ag atoms interact only weakly with the Si(111)- 2×1 surface, that is, at such a low temperature the Ag atoms are physisorbed and not chemisorbed. In fact, during deposition on the substrate at low temperatures the Si(111)- 2×1 substrate pattern can be observed (at a primary electron energy $\varepsilon \approx 100$ eV) up to a coverage $\theta \approx 3-4$, that is, with allowance for the coefficient α , up to about a coverage of 1.5-2 layers of silver atoms. We emphasize that as θ increases the superstructure beams and the main beams disappear practically simultaneously (the main beams being those from the Si(111)- 1×1 structure). Because in the LEED experiments only the elastically scattered electrons are detected, it is clear that the disappearance of all the LEED beams from the Si(111) surface at $\theta \approx 3$ means that the Ag film for $\theta \approx 3$ is opaque to the electrons of energy $\varepsilon \approx 100$ eV that are detected: all the electrons with $\varepsilon \approx 100$ eV that are incident on the Ag film are inelastically scattered with high probability and therefore do not contribute to the LEED pattern. Consequently, from the LEED data we can estimate, albeit crudely, the mean free path without energy loss for a 100 eV electron. It is clear that $1 \lesssim \theta \lesssim 3$. If the coefficient α is taken into account, then this value agrees with the value for the electron mean free path that we obtained from the experimental EAS data.

The complete absence of diffracted beams from Ag(111) for $\theta \lesssim 3-4$ or the presence of only very diffuse beams (spots) for $\theta \gtrsim 3-4$ with the spots as large as the spacing between them, indicate that the Ag atoms that are adsorbed at 8 K form a highly disordered structure.

Knowing the size Δq_{Ag} of the Ag(111) beams observed during the process of deposition at 8 K ($\theta \gtrsim 3-4$) and the lattice constant a_{Ag} in the Ag(111) plane, one can estimate the short range order length in the system of Ag atoms as $\xi \sim (q_{\text{Ag}}/\Delta q_{\text{Ag}})a_{\text{Ag}}$, where q_{Ag} is the spacing between the Ag diffracted beams. In our case, $\xi \approx (2-3)a_{\text{Ag}}$ for $\theta \gtrsim 3-4$. We stress that because the diffuseness of the diffracted beams decreases and their intensities increase with increasing θ (for $\theta \gtrsim 3-4$) we can conclude that, first, the Ag film produced at 8 K is nearly amorphous, and second, the degree of ordering in deposition at 8 K increases with increasing film thickness.

We thus arrive at the conclusion that in the low-temperature adsorption of Ag on the Si(111)- 2×1 surface an Ag film with $\xi \lesssim (2-3)a_{\text{Ag}}$ is formed which interacts weakly

with the substrate and that the experimentally determined dependences $I_{\text{Si}}(\theta)$ and $I_{\text{Ag}}(\theta)$ are very well described within the Poisson statistical model with a single adjustable parameter $l(\varepsilon)$ for all the values of θ that were studied.

We shall now discuss briefly the results of the room temperature experiments. As can be seen from Figs. 2 and 3 (see also Refs. 17 and 19) there are breaks in the experimental curves of $I_{\text{Si}}(300 \text{ K}, \theta)$ and $I_{\text{Ag}}(300 \text{ K}, \theta)$ corresponding to $\theta \approx 1$. We can therefore state that $\theta \approx 1$ is a critical coverage and we designate this coverage θ_c . This observation also agrees qualitatively with data obtained by the LEED method. Actually, as the LEED experiments show, the formation of a new superstructure, the $\text{Si}(111)\text{-}\sqrt{7} \times \sqrt{7}R(\pm 19.1^\circ)$ is completed on the $\text{Si}(111)$ surface at $\theta \approx \theta_c \approx 1.2\text{--}1.3$. We note that in Ref. 17 a critical coverage $\theta_c \approx 0.66$ was obtained. The reason for the substantial discrepancy with our result $\theta_c \approx 1.2\text{--}1.3$ is not clear.

Worthy of note is the fact that the curves of $I_{\text{Ag}}(\theta)$ for $T = 8$ and $T = 300 \text{ K}$ coincide (within experimental error) over the entire range of θ from 0 to ≈ 1 . This result permits us to assume that at 300 K and 8 K the Ag atoms are localized on the surface and not beneath the upper layer of Si atoms (as occurs for $T \gtrsim 300 \text{ K}$ (Ref. 13)), that is, there is no appreciable intermixing of Ag and Si atoms. We note that for $\theta \ll 1$ the probability of Ag atoms lying on top of one another, and, consequently, the possibility of their mutual screening, is small. Therefore it is reasonable to expect that at 8 K in the range $\theta \leq 1$ the condition $I_{\text{Ag}}(300 \text{ K}) \approx I_{\text{Ag}}(8 \text{ K})$ should hold, since for $\theta \leq 1$ the atoms form mainly monolayer islands with the $\sqrt{7} \times \sqrt{7}$ structure, that is, the Ag atoms are arranged in a single plane on the surface (see below).

Let us now take note of the fact that at 300 K in the region $\theta < 1$ the dependence $I_{\text{Si}}(\theta)$ is steeper than the curve for 8 K (see Fig. 2) particularly for $\theta \rightarrow 0$.

$$\partial I_{\text{Si}}(300 \text{ K}, \theta) / \partial \theta \approx 1.2 \partial I_{\text{Si}}(8 \text{ K}, \theta) / \partial \theta.$$

Taking into account also that at 300 K the intensities of the $\sqrt{7} \times \sqrt{7}$ superstructure diffracted beams increase monotonically with θ up to $\theta \approx 1.2\text{--}1.3$, it is reasonable to suppose that the steeper dependence $I_{\text{Si}}(300 \text{ K}, \theta)$ is due to the more effective scattering of electrons by the essentially monolayer Ag islands which are formed and grow in breadth with increasing θ . (We note that even at $\theta \approx 1$ about 37% of the surface is not covered by the adsorbate in a statistical distribution of the atoms, and therefore the effectiveness of screening of the Si Auger electrons is reduced). At 300 K in each island that is investigated the concentration of Ag atoms clearly corresponds to $\theta_c \approx 1$, and the superstructure is the $\sqrt{7} \times \sqrt{7}$ structure.

We shall assume that the concentration of adatoms between the islands can be neglected. Then we can write that

$$I_{\text{Si}}(300 \text{ K}, \theta) = I_0(S_0 - S) + I_0 S \exp(-d^*/l^*),$$

where I_0 is the intensity of the Auger signal for the clean surface, d^* and l^* are, respectively, the effective thickness and electron mean free path for islands with the $\sqrt{7} \times \sqrt{7}$ structure, S_0 is the surface area of the sample, and S is the

total area of all the islands with the $\sqrt{7} \times \sqrt{7}$ structure. In this case the measured coverage is $\theta = \theta_c S / S_0$; at $S = S_0$ the entire surface is covered with a Ag layer with $\theta = \theta_c$ that has the $\sqrt{7} \times \sqrt{7}$ structure. Consequently, for $\theta < 1$ we have

$$I_{\text{Si}}(300 \text{ K}, \theta) = I_0 S_0 \{1 + [\exp(-d^*/l^*) - 1] \theta / \theta_c\},$$

that is, the dependence on θ is linear, in accordance with Fig. 2. From this result we find that for $\theta < 1$,

$$\frac{1}{I_0 S_0} \frac{\partial I_{\text{Si}}(300 \text{ K}, \theta)}{\partial \theta} = \frac{1}{\theta_c} \left[\exp\left(-\frac{d^*}{l^*}\right) - 1 \right].$$

From Fig. 2 we find that the left hand side of this expression (e) is equal numerically to ≈ -0.4 , and therefore, setting $\theta_c \approx 1$, we obtain $d^*/l^* \approx 0.5$. We emphasize that we cannot separately determine the mean free path l^* for the $\sqrt{7} \times \sqrt{7}$ superstructure because the effective thickness d^* is unknown.

Let us now consider the coverage range $\theta \gtrsim 1$. The fact that for $\theta \gtrsim 1$ all the experimental points of the curve $I_{\text{Ag}}(300 \text{ K}, \theta)$ lie below those for $I_{\text{Ag}}(8 \text{ K}, \theta)$ indicates that at 300 K, as θ increases over the range $\theta \gtrsim 1$, three-dimensional islands of Ag are formed on top of the first monolayer (which forms the $\text{Si}(111)\text{-}\sqrt{7} \times \sqrt{7}R(19.1^\circ)$ superstructure). This conclusion is consistent with the data of Fig. 2. Actually, as can be seen from Fig. 2, for $\theta \gtrsim 1$ the dependence on θ of $I_{\text{Si}}(300 \text{ K}, \theta)$ is weaker than that of $I_{\text{Si}}(8 \text{ K}, \theta)$, a result that also is evidence for the growth of three-dimensional islands on top of the first Ag monolayer (the Stranski-Krastanov mechanism).

This conclusion is also supported by the LEED results. In the experiments, deposition at room temperature to $\theta \sim 20$ does not extinguish the $\text{Si}(111)\text{-}1 \times 1$ pattern. Since the mean free path of the electrons is $l \approx 3$ monolayers, it is clear that for a uniform coverage at room temperature the $\text{Si}(111)\text{-}1 \times 1$ LEED pattern would disappear at $\theta \approx 3$, as occurs in the case of deposition at 8 K. Consequently, there is basis for the conclusion that after formation of the first monolayer at $T \approx 300 \text{ K}$ (see also below), three-dimensional (3D) islands subsequently form and grow over the entire surface on top of the two-dimensional layer up to $\theta \approx 20$. Between the 3D islands regions of the two-dimensional layer remain, and these are transparent to electrons of energy $\varepsilon \approx 100 \text{ eV}$. The $\text{Si}(111)\text{-}1 \times 1$ structure can be seen through these regions.

When the samples that were prepared by deposition at 8 K were heated to $T \gtrsim 100 \text{ K}$ we observed that for $\theta \gtrsim \theta^*$, where θ^* is some critical coverage around 0.4–0.5, an irreversible phase transition, $\text{Si}(111)\text{-}2 \times 1 \rightarrow \text{Si}(111)\text{-}1 \times 1$, occurred on the surface. (This was manifested in the disappearance of the superstructure diffracted beams). Moreover, the temperature of this transition depended strongly on the coverage, and decreased with increasing coverage θ . The disappearance of the superstructure diffracted beams upon heating can be interpreted as being a consequence of the strengthening of the interaction of the adsorbed Ag with the $\text{Si}(111)$ surface in the transition from the physisorbed to the chemisorbed, i.e., the strongly bound, state. This transition is a thermally activated process. This

conclusion is in agreement with the results of Ref. 33. Strengthening of the interaction leads to a local disruption of the translational symmetry corresponding to the superstructure. It is important to point out that for the "removal" of the 2×1 superstructure at $T \gtrsim 100$ K it is necessary that $\theta \gtrsim \theta^* \approx 0.4-0.5$.

From the value of θ^* we can estimate the characteristic radius of interaction of the Ag atoms in the chemisorbed state with the Si atoms. It is evident that $r \sim 1/2(\theta^*)^{-1/2}a_{\text{Si}}$, where a_{Si} is the lattice constant on the Si(111) surface. Setting $a_{\text{Si}} \approx 3.84$ Å, we find that $r \approx 3$ Å. It is clear that the critical value θ^* must be a universal characteristic, essentially independent of the temperature. However, we have determined that the value of θ at which all the diffracted beams from the 2×1 superstructure disappear during deposition at room temperature is about equal to 2 (see also Refs. 17 and 19), and not 0.4–0.5. We therefore arrive at the conclusion that at room temperature, because of rapid surface diffusion, compact two-dimensional Ag islands form immediately and grow laterally (without changing thickness) and gradually cover the whole surface. During this process the concentration of Ag atoms in the islands is $\gtrsim \theta^*$ and therefore under the islands we have the Si(111)- 1×1 structure while between the islands $\theta < \theta^*$ and, as a consequence, in these nearly "clean" regions of the surface the Si(111)- 2×1 superstructure persists. The total disappearance of the Si(111)- 2×1 superstructure diffraction beams corresponds, in this model, to the enlargement of the two-dimensional islands. This disappearance corresponds to $\theta \approx 2$, since $\alpha \approx 0.56$ (see above). This proposed growth mechanism is also supported by the LEED data.

The results that we have obtained in experiments on heating samples of "thick" Ag films ($\theta \gtrsim 3-4$) deposited at 8 K also serve as confirmation of the proposed mechanism. In this case, when the samples are heated to $T \gtrsim 100$ K we observe a transition—(nonuniform background) \rightarrow Ag(111)- $1 \times 1 +$ Si(111)- 1×1 —which can also be interpreted as resulting from the transformation into islands of a film that is initially continuous at 8 K. This conclusion is in good agreement with our conclusions drawn on the basis of an analysis of the Auger data. Both our LEED and AES results show that at low temperatures (≈ 8 K) during the deposition of Ag on the Si(111)- 2×1 surface a continuous film grows, with a statistical distribution of the silver atoms over the thickness of the film. On the other hand, room temperature growth of the film occurs by the Stranski-Krastanov mechanism.

Thus, on the basis of an analysis of the experimental data we have arrived at a number of hypotheses and conclusions regarding physisorption and chemisorption, the mean free path l in a Ag film for electrons of energy $\varepsilon \approx 100$ eV, the characteristic radius r of interaction of Ag atoms with Si atoms on the Si(111) surface, and the growth mechanism of Ag films at low and room temperatures. The conclusions on the growth mechanisms of Ag films on the Si(111)- 2×1 surface at low and room temperatures are in good accord with the results obtained on heating the films to room temperature. It can be seen from Fig. 4 that for $\theta > 1$ the ratio

$I_{\text{Ag}}/I_{\text{Si}}$ decreases in the process of heating to room temperature. Heating to ≈ 100 K, regardless of the coverage θ , produces no marked change in $I_{\text{Ag}}/I_{\text{Si}}$. Therefore there is reason to suppose that there is essentially no surface diffusion of Ag atoms or segregation into islands in the temperature range 8–100 K. On the other hand, the Ag atoms begin to diffuse noticeably over the surface at $T \gtrsim 100$ K and to collect into islands. When this happens, some portions of the surface are "cleaned" of the silver film and the measured Auger signal from the silver decreases and that from the silicon increases. The final value of $I_{\text{Ag}}/I_{\text{Si}}$ is that which is obtained in room temperature deposition to the same coverage θ .

During the heating of samples with $\theta \gtrsim 0.7$ the Ag(111)- 1×1 diffracted beams begin to form already at $T \gtrsim 100$ K. The formation of these beams in the shape of an arc indicates that in the system of Ag atoms, which is initially highly disordered, ordered regions appear in which the axes of the type $\langle 111 \rangle$ practically coincide with the $\langle 111 \rangle$ axis of the substrate, but with a large spread in the angles of rotation φ of these regions relative to each other around the $\langle 111 \rangle$ axis (up to $\Delta\varphi \approx \pm 5^\circ$). We note that the radial diffuseness Δq_{Ag} decreases with increasing T .

The data from the heating experiments allow us to conclude that the films that are prepared at low temperatures and have a statistical distribution of the Ag atoms over the thickness of the film form into islands when heated. When they are heated to room temperature they evidently have nearly the same structure as films deposited at room temperature to the same coverage θ .

We note that the reason for the very strong film thickness dependence of the temperature at which the structural rearrangement begins upon heating the sample remains essentially unclear. Additional investigations are required to clarify this point.

In connection with our observation of the Si(111)- 3×1 LEED pattern, there are two possible reasons for its appearance. First, this pattern may result from the formation of a 3×1 superstructure involving Ag atoms, i.e., a Si(111)- 3×1 -Ag superstructure, and the diffraction of the primary electron from this superstructure. Second, it could be, generally speaking, a result of the difference, by a factor of about 1/3, in the lattice constants a_{Si} and a_{Ag} in the (111) plane, by virtue of which LEED superstructure diffraction beams, spaced a distance $q_{\text{Si}}/3$ apart (see Sec. III), can arise by diffraction, not of the primary beam, but of the beams diffracted by the Si and passing through the Ag film from the reverse side (the double diffraction effect³³). It is clear that the doubly diffracted beams can leave the Ag film and reach the LEED screen only if the thickness of the film is less than or equal to l , the mean free path of 100 eV electrons.

The following facts are also evidence in favor of double diffraction.

If the LEED pattern is observed during room temperature deposition, then the 3×1 diffraction beams appear at approximately the same coverage as the Ag(111)- 1×1 pattern (see Table I). The same is true of the films that are prepared at 8 K and then heated. At the same time, in the

case of deposition at ~ 300 K, the 3×1 structure disappears for large θ when the silver islands become sufficiently thick and consequently opaque to the electrons emerging from the silicon with an energy $\varepsilon \approx 100$ eV. Furthermore, we note that for low temperature deposition the film that is obtained is highly disordered and therefore up to large coverages we observe diffracted beams from neither the $\text{Ag}(111)-1 \times 1$ nor the 3×1 structures. Briefly generalizing the observation discussed above, we may say that the 3×1 structure appears and exists simultaneously with the $\text{Ag}(111)-1 \times 1$ structure if the film is sufficiently thin, and it disappears at large θ .

In spite of all the arguments given above in favor of the 3×1 structure being a double diffraction phenomenon, we suggest that additional studies are necessary for a final explanation of its nature.

V. CONCLUSIONS

The experimental investigations that we have carried out over a wide temperature range by the methods of low energy electron diffraction and Auger electrons spectroscopy have made it possible for the first time to obtain a body of data on the growth kinetics of ultrathin Ag films, on the atomic structure of the Si(111) surface as the concentration of adsorbed Ag atoms is varied at low temperatures, and on the effect of temperature on the structure of the Si(111) surface and the Ag film.

A comparison of the low temperature results and the results obtained at room temperature have allowed us to form hypotheses about the specific growth mechanisms of the Ag films and about the nature of the interaction between the Ag atoms and the Si(111) surface at various temperatures. An analysis of the experimental data has also allowed us to determine the mean free path of electrons with energies 92 eV and 356 eV in the Ag films. We point out that the determination of the mean free path by deposition of films at low temperatures is the more correct way in the sense that at low temperatures there are no problems associated with the formation of island structures.

The body of experimental results that was obtained indicates that at low temperatures there are a number of interesting phenomena in the Si(111)-Ag system that warrant further investigation. For instance, an interesting feature is the observation of an amorphized Ag film on the Si(111) surface. This observation is evidently the first of its kind and it merits further attention.

The authors wish to express their gratitude to A. M.

Ionov for helping in building the apparatus for the low-temperature, ultrahigh-vacuum investigations.

- ¹G. Le Lay, *Surf. Sci.* **132**, 169 (1983).
- ²Y. Horio and A. Ichimiya, *Surf. Sci.* **133**, 393 (1983).
- ³K. Horioka, H. Iwasaki, S. Maruno S. Te Li, and S. Nakamura, *Solid State Commun.* **47**, 55 (1983).
- ⁴S. Kono, H. Sakurai, K. Higashiyama, and T. Sagawa, *Surf. Sci.* **130**, L299 (1983).
- ⁵T. Yokotsuka, S. Kono, S. Suzuki, and T. Saiyawa, *Surf. Sci.* **127**, 35 (1983).
- ⁶J. Stohr, R. Jaeger, G. Rossi, T. Kendelewicz, and I. Lindau, *Surf. Sci.* **134**, 813 (1983).
- ⁷A. L. Wachs, T. Miller, and T. C. Chiang, *Phys. Rev. B* **29**, 2286 (1984).
- ⁸M. Hanbücken, M. Futamoto, and J. A. Venables, *Surf. Sci.* **147**, 433 (1984).
- ⁹S. Nishigaki, K. Takao, T. Yamada, M. Arimoto, and T. Komatsu, *Surf. Sci.* **158**, 473 (1985).
- ¹⁰E. J. Van Loenen, M. Iwami, R. M. Tromp, and J. F. Van der Veen, *Surf. Sci.* **137**, 1 (1984).
- ¹¹J. E. Demuth and B. N. J. Persson, *Appl. Surf. Sci.* **22/23**, 415 (1985).
- ¹²K. Spiegel, *Surf. Sci.* **7**, 125 (1967).
- ¹³M. Saitoh, F. Shoji, K. Oura, and T. Hanawa, *Jpn. J. Appl. Phys.* **19**, L421 (1980).
- ¹⁴V. G. Lifshitz, *Elektronnaya Spektroskopiya i Atomnye Protsessy na Poverkhnosti Kremniya* [Electron Spectroscopy and Atomic Processes on Silicon Surfaces], Nauka, Moscow (1985).
- ¹⁵J. Derrien, G. Le Lay, and F. Salvan, *J. de Phys. Lett.* **39**, L287 (1978).
- ¹⁶A. McKinley, R. H. Williams, and A. W. Parke, *J. Phys. C* **12**, 2447 (1979).
- ¹⁷D. Bolmont, Ping Chen, C. A. Sebenne, and F. Proix, *Phys. Rev. B* **24**, 4552 (1981).
- ¹⁸G. Rossi, I. Abbati, I. Lindau, and W. E. Spicer, *Appl. Surf. Sci.* **11/12**, 348 (1982).
- ¹⁹G. Le Lay, A. Chouvet, M. Manneville, and R. Kern, *Appl. Surf. Sci.* **9**, 190 (1981).
- ²⁰A. Thanailakis, *J. Phys. C* **8**, 655 (1975).
- ²¹J. D. Van Otterloo and J. G. De Groot, *Surf. Sci.* **57**, 96 (1976).
- ²²G. Le Lay, *J. Vac. Sci. Technol. B* **1**, 354 (1983).
- ²³G. Le Lay, G. Quentel, J. P. Faurie, and A. Masson, *Thin Solid Films* **35**, 273 (1976).
- ²⁴G. Dufour, J. M. Mariot, A. Masson, and H. Roulet, *J. Phys. C* **14**, 2539 (1981).
- ²⁵Che Jinguang, Zhang Kaiming, and Xie Xide, in: *Proc. of the 17th Intern. Conf. on the Physics of Semiconductors*, San Francisco, 1984; Eds: J. D. Chadi and W. A. Harrison, Springer Verlag, New York, Berlin, Heidelberg, 1985, p. 121.
- ²⁶A. G. Naumovets and Yu. S. Vedula, *Surf. Sci. Rep.* **4**, 365 (1984).
- ²⁷V. Yu. Aristov, N. I. Golovko, V. A. Grazhulis, Yu. A. Ossipyan, and V. I. Talyanskii, *Surf. Sci.* **117**, 204 (1982).
- ²⁸D. Haneman, and R. Z. Bachrach, *J. Vac. Sci. Technol.* **21**, 337 (1982).
- ²⁹V. Yu. Aristov, I. E. Batov, and V. A. Grazhulis, *Surf. Sci.* **132**, 73 (1983).
- ³⁰A. S. Novik *Comments Solid State Phys.* **2**, 155 (1970).
- ³¹V. M. Kuz'menko, B. G. Lazarev, V. I. Mel'nikov, and A. I. Sudovtsev, *Ukr. Fiz. Zh.* **21**, 881 (1976).
- ³²G. Rossi, I. Abbati, L. Braicovich, I. Lindau, and W. E. Spicer, *Surf. Sci.* **112**, L765 (1981).
- ³³Y. Terada, T. Yoshizuka, K. Oura, and T. Hanawa, *Surf. Sci.* **114**, 65 (1982).

Translated by J. R. Anderson